Electrical resistivity, electronic heat capacity, and electronic structure of Gd_5Ge_4

E. M. Levin,[1] V. K. Pecharsky,[1,2,*] K. A. Gschneidner, Jr.,[1,2] and G. J. Miller[3]
[1]*Ames Laboratory, Iowa State University, Ames, Iowa 50011-3020*
[2]*Department of Materials Science and Engineering, Iowa State University, Ames, Iowa 50011-3020*
[3]*Department of Chemistry, Iowa State University, Ames, Iowa 50011-3020*
(Received 16 May 2001; published 8 November 2001)

Temperature and dc magnetic-field dependencies of the electrical resistivity (4.3–300 K, 0–40 kOe) and heat capacity (3.5–14 K, 0–100 kOe) of polycrystalline Gd_5Ge_4 have been measured. The electrical resistivity of Gd_5Ge_4 shows a transition between the low-temperature metallic and high-temperature insulatorlike states at ~130 K. In the low-temperature metallic state both the resistivity and electronic heat capacity of Gd_5Ge_4 indicate a possible presence of a narrow conduction band. Both low- and high-temperature behaviors of the electrical resistivity of Gd_5Ge_4 correlate with the crystallographic and magnetic phase transitions induced by temperature and/or magnetic field. Several models, which can describe the unusual behavior of the electrical resistance of Gd_5Ge_4 above 130 K, are discussed. Preliminary tight-binding linear muffin-tin orbital calculations show that Gd_5Ge_4 behaves as a metal in the low-temperature magnetically ordered state, and as a Mott-Hubbard ''semiconductor'' in the high-temperature magnetically disordered state.

DOI: 10.1103/PhysRevB.64.235103 PACS number(s): 72.15.Eb, 72.15.Rn, 65.40.Ba, 71.20.−b

I. INTRODUCTION

The electrical resistivity (ρ) of rare-earth-based intermetallics without an energy gap in the electronic structure, in general, and silicides and germanides, in particular, is determined by several contributions which arise from phonon, electron, magnetic, and other scattering mechanisms.[1,2] Correspondingly, when any or all of these interactions change significantly, e.g., during magnetic phase transformations between different magnetically ordered phases, or between magnetically ordered and disordered phases, an anomalous behavior of the electrical resistivity is usually observed. In multidomain ferromagnetic materials, an additional contribution to the resistivity arises from domain walls when compared to a single-domain ferromagnet.[3]

In lanthanide-based materials, f-$s(d)$ interactions play an important role in determining the behavior of their electrical resistivity.[1] Because $4f$ electronic states are well localized, the exchange interactions in the lanthanide-based intermetallic compounds are generally described by the Ruderman-Kittel-Kasuya-Yosida model, which is based on the interactions between the localized $4f$-electron magnetic moments and the $s(d)$ conduction electrons. Hence, the electronic transport in $4f$ systems is sensitive to the f-$s(d)$ interactions and in some materials, e.g., Kondo systems, these interactions can be strong enough to create heavy fermion state and induce a narrow energy gap at Fermi level.[1,4] Therefore, the behavior of the electrical resistivity in lanthanide-based materials, especially those with first- and (or) second-order phase transitions, can be quite complex, but it provides a useful indicator enabling a better understanding of the electronic processes as the temperature and/or magnetic field vary.

The electrical resistivity of the Gd-based intermetallic alloys, including complex silicides[2,5] and germanides,[6] usually shows a positive $d\rho/dT$. However, in some lanthanide-based materials the resistivity may show a negative $d\rho/dT$ due to different reasons [for example, above the Néel temperature in Gd_2CuGe_3,[6] or in the vicinity of the magnetic phase transformations in Gd_2In (Ref. 7)] indicating the presence of weak conduction-electron localization effects. The electrical resistivity in these cases is mainly determined by correlation between the localized $4f$ electronic states and conduction electrons.

In other systems, e.g., in the $Gd_5(Si_xGe_{4-x})$ alloys, the nature of electron correlations is largely affected by a specific change of the electronic, magnetic, and crystal structures, and significant anomalies of the electrical resistivity are found during the first-order magnetic phase transitions induced by temperature and/or magnetic field.[8–10] These alloys are based on Gd_5Ge_4 and Gd_5Si_4 compounds which were thought to have the same crystal structure,[11] but later were found to have distinct differences in Si-Si and Ge-Ge bonding.[12,13] It was reported that Gd_5Ge_4 is a simple antiferromagnet with a Néel temperature of ~15 K.[11] However, our study[14] showed that this binary compound has a much more complex temperature and magnetic field dependence of its magnetic state.

Gd_5Ge_4 has a distinctly layered crystal structure (Fig. 1) where four monoatomic, almost flat, layers formed by either Gd or Ge atoms, and one mixed (Gd+Ge) atomic layer are tightly bonded together, thus creating two-dimensional slabs. At room temperature, when the compound is paramagnetic, the slabs are not connected with one another via covalentlike Ge-Ge bonds.[12] As shown by Choe *et al.*,[13] the crystallographic phase transformation in $Gd_5(Si_2Ge_2)$ is accompanied by a breaking and reforming of one-half of the interslab bonds. Recently, Morellon *et al.*[15] also reported a similar crystallographic transformation in $Gd_5(Si_{0.4}Ge_{3.6})$, and an analysis of their crystallographic data indicates that all interslab bonds break and reform during the crystallographic transition in $Gd_5(Si_{0.4}Ge_{3.6})$. We note that crystallography and magnetism in the $Gd_5(Si_xGe_{4-x})$ system are closely related, i.e., in all alloys studied to date,[8–15] the *ferromagnetic state is observed only when all slabs are interconnected* [the

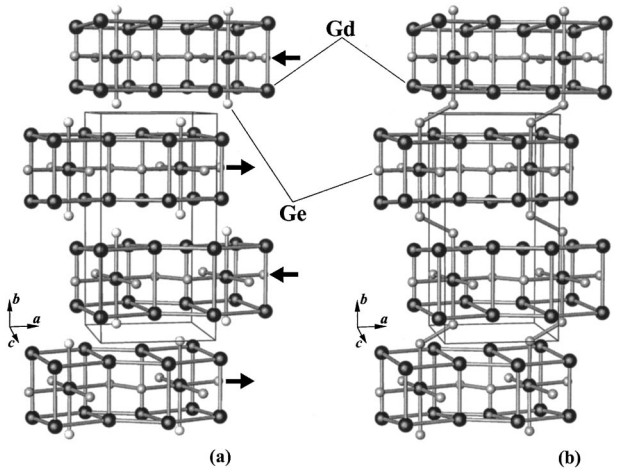

FIG. 1. The crystal structures of Gd_5Ge_4 in the room-temperature paramagnetic state and low-temperature antiferromagnetic states (a) and in the low-temperature ferromagnetic state (b). The essentially identical slabs are formed from cubes and trigonal prisms with Gd atoms in all corners sharing rectangular faces, and include $GdGe_6$ octahedra. The directions, in which the slabs move relative to one another during the antiferromagnetic-ferromagnetic phase transition, are shown by thick horizontal arrows in (a). The short Ge-Ge distances corresponding to the covalentlike interslab Ge-Ge bonding in the ferromagnetic state are shown in (b) by a thick line connecting the corresponding Ge atoms. This model is based on the crystallographic results given in Refs. 11–13 and 15.

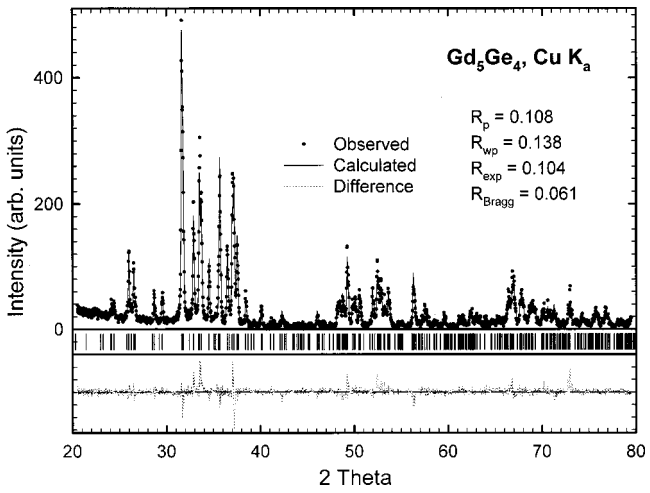

FIG. 2. The observed (dots) and calculated (line) diffraction patterns of the as-arc-melted Gd_5Ge_4 alloy. The x-ray-diffraction data were collected at room temperature. Vertical lines at the bottom of the plot indicate the calculated ($\lambda K_{\alpha 1}$) positions of the Bragg peaks.

Gd_5Si_4-type structure; see Fig. 1(b)], while the paramagnetic state exists when none [Sm_5Ge_4-type structure; see Fig. 1(a)], one-half [$Gd_5(Si_2Ge_2)$-type structure[13]], or all (Gd_5Si_4-type structure[12]) slabs are interconnected.

In this paper we report on the temperature (4.3–300 K) and magnetic field (0–40 kOe) dependencies of the electrical resistivity and the temperature (3.5–14 K) and magnetic field (0–100 kOe) dependencies of the electronic heat capacity of polycrystalline Gd_5Ge_4, and on the results of tight-binding linear-muffin-tin-orbital calculations of its electronic band structure.

II. EXPERIMENTAL DETAILS

The Gd_5Ge_4 compound was prepared by arc melting a stoichiometric mixture of the constituent elements using Gd (99.9-at. % purity) and Ge (99.99-at. % purity). Gadolinium was prepared by the Materials Preparation Center, Ames Laboratory, and contained the following major impurities (in ppm atomic): O, 440; C, 200; H, 160; N, 90; Fe, 40; and F, 30. Germanium was purchased from CERAC, Inc. The alloy (total weight ~15 g) was arc melted six times, with the button being turned over each time to ensure alloy homogeneity. Weight losses during arc melting were negligible, and, therefore, the alloy composition was assumed to remain unchanged. No impurity phases were detected by x-ray powder diffraction (see the results of Rietveld refinement in Fig. 2) and optical metallography; therefore, the alloy was studied without further heat treatment. The crystal structure of the prepared Gd_5Ge_4 is orthorhombic, space group *Pnma* with the following lattice parameters: $a=7.6968(5)$ Å, $b=14.831(1)$ Å, and $c=7.7851(5)$ Å, i.e., the same as reported earlier.[12]

The polycrystalline sample for the electrical measurements had the dimensions $\sim 2\times 2\times 4$ mm^3. Electrical connections to the sample were made by attaching thin platinum wires using H20E Epotek silver paste manufactured by Epoxy Technology. The dc electrical resistance measurements were carried out using Lake Shore Model No. 7225 magnetometer equipped with a probe for making four-point measurements. The measurements were performed at a constant dc electrical current of 10 mA in a temperature range from 4.3 to 300 K and in magnetic fields from 0 to 40 kOe with the current applied in opposite directions to eliminate possible thermals. The magnetic-field vector was oriented parallel to the direction of electrical current **j**. The heat capacity was measured using an automatic adiabatic heat pulse calorimeter.[16] The polycrystalline sample for the heat capacity measurements was $\sim 10\times 10\times 3$ mm^3. The electronic heat capacity (γ) was determined by fitting the low temperature data to the expression $C=\gamma T+\beta T^3$, where C is the molar heat capacity, β is the lattice heat capacity, and T is the absolute temperature. The error of resistance measurements was ~1%, heat capacity ~0.7%. The details of the calculations of the electronic structure of Gd_5Ge_4 will be presented below (see Sec. III E).

III. EXPERIMENTAL RESULTS AND DISCUSSION

A. Electrical resistance

Temperature dependencies of the electrical resistivity of Gd_5Ge_4, measured on heating and cooling between 4.3 and 300 K, are shown in Fig. 3. The measurement on heating was made after the sample was slowly (~0.5 K/min) cooled in the zero magnetic field. Both resistivity functions of Gd_5Ge_4

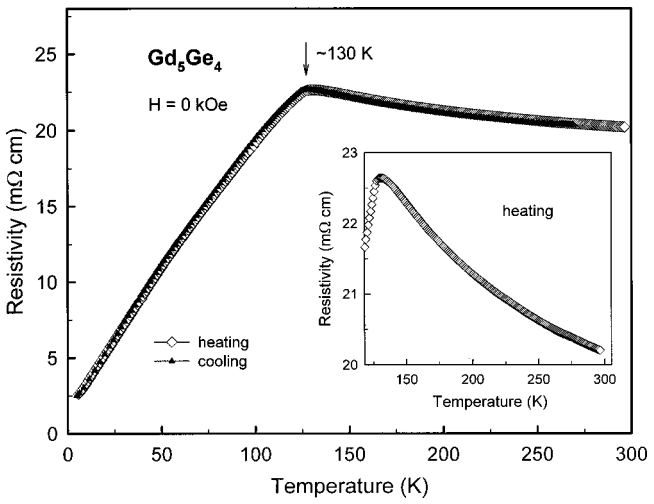

FIG. 3. Temperature dependencies of the electrical resistivity of polycrystalline Gd_5Ge_4 measured on heating and cooling in zero magnetic field. The inset shows an expanded view of the behavior above 120 K.

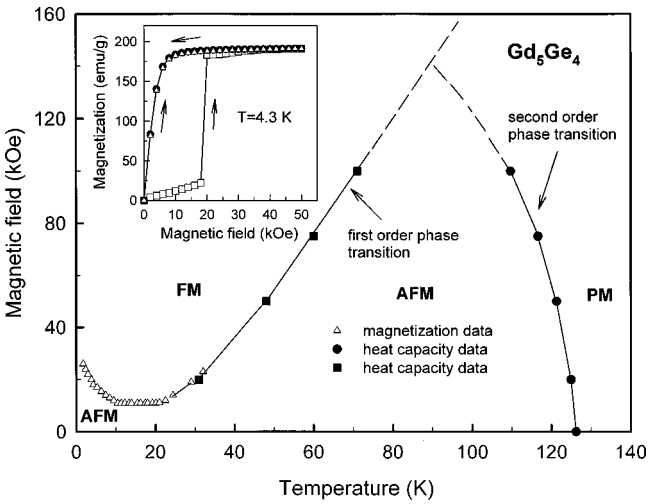

FIG. 4. The magnetic phase diagram of Gd_5Ge_4, which was constructed from the heat capacity and magnetization data, delineates the phase fields observed in the system during isofield heating or isothermal magnetizing. The inset shows the magnetization of Gd_5Ge_4 cooled in zero magnetic field. During the first magnetic field increase, which is shown by open squares in the inset, a metamagneticlike transition occurs at ~18 kOe. During the first magnetic-field reduction (closed circles) and during the second and following magnetic-field increases (opened triangles), the magnetization behavior is typical of a soft ferromagnet.

in zero magnetic field show the same behavior, indicating that the mechanisms of charge-carrier scattering and their concentration, if any, are independent of the direction of the temperature change. The electrical resistivity exhibits the low-temperature metallic and the high-temperature semiconductorlike behaviors, and displays a well-defined peak at ~130 K; see the inset in Fig. 3. In general, the character of the temperature dependence of the resistivity of Gd_5Ge_4 between 5 and 300 K is similar to that reported in Ref. 17, but the resistivity values—the $\Delta\rho/\rho\Delta T$ ratio in the metallic state, the temperature of the peak, and the behavior of ρ above 130 K—are different. According to our data, the resistivity of our Gd_5Ge_4 sample is approximately 2.6 and 22.6 $m\Omega\,cm$ at 5 and 130 K, respectively, and the $\rho_{130\,K}/\rho_{5\,K}$ ratio is 8.7. Reference 17 reported a resistivity maximum of 32 $m\Omega\,cm$ at 115 K and a $\rho_{115\,K}/\rho_{5\,K}$ ratio of about 2.1. In both cases, a large resistivity of Gd_5Ge_4 at 5 K reflects the presence of microcracks in the sample, which is typical of all $Gd_5(Si_xGe_{4-x})$ alloys.[8,9] Between 10 and 50 K, the electrical resistivity of Gd_5Ge_4 shows nearly linear ($\rho \propto BT$) dependence with $B = 186\ \mu\Omega$ cm/K. Based on the observed change of the electrical resistivity behavior from metalliclike to superconductorlike i.e., a change of the sign of $d\rho/dT$ from positive to negative, it is feasible that a metal-insulator transition MIT[18] takes place in Gd_5Ge_4 at ~130 K. Although the observed behavior of the electrical resistivity is obviously nonrepresentative of a MIT, we used this term to indicate that the varying temperature induces a transition between the metallic and nonmetallic behaviors in Gd_5Ge_4.

The observed behavior of the electrical resistivity is closely related to the magnetic state of Gd_5Ge_4 as a function of both temperature and magnetic field. Full details about the magnetism of the Gd_5Ge_4 system will be published elsewhere,[14] but a brief description of the most important results is given below. As shown in Fig. 4, above ~130-K Gd_5Ge_4 is paramagnetic, while below 130 K the Gd sublattice in the Gd_5Ge_4 compound cooled at zero magnetic field forms an unusual antiferromagnetic (AFM) structure, possibly one of the few types discussed in Ref. 19. No ferromagnetic order has been detected in zero magnetic field down to the lowest available temperature, ~1.8 K. The application of a magnetic field exceeding ~18 kOe at 4.3 K transforms the AFM state in Gd_5Ge_4 into a ferromagnetic (FM) state similar to that usually observed during metamagnetic transitions (see the inset in Fig. 4). Although no direct confirmation exists so far for this material, we believe that the AFM→FM transition in Gd_5Ge_4, induced by a magnetic field, is accompanied by a crystallographic Sm_5Ge_4-type→Gd_5Si_4-type transition as shown in Fig. 1 and reported for $Gd_5(Si_{0.4}Ge_{3.6})$ in Ref. 15. After the magnetic field is reduced isothermally back to zero, Gd_5Ge_4 remains in the FM state (see the inset in Fig. 4). The inverse FM→AFM transformation in Gd_5Ge_4 can be induced only by heating the sample from 4.3 K to above ~25 K. Above ~25 K, the combined AFM↔FM and crystallographic (Fig. 1) transformations can be induced reversibly by the isothermal application and removal of the magnetic field; therefore, this behavior is similar to that observed in other of $Gd_5(Si_xGe_{4-x})$ materials.[8,9] Hence the high-temperature nonmetallic state of Gd_5Ge_4 is magnetically disordered, the low-temperature (zero magnetic field) metallic state is antiferromagnetic, and the combined magnetic-crystallographic transition is irreversible below ~10 K but becomes fully reversible above ~25 K. We note that according to the heat-capacity data the high-temperature AFM↔PM transformation is a second-order phase transition, and the low-temperature magnetic AFM↔FM and crystallographic transformations are first-order phase transitions.

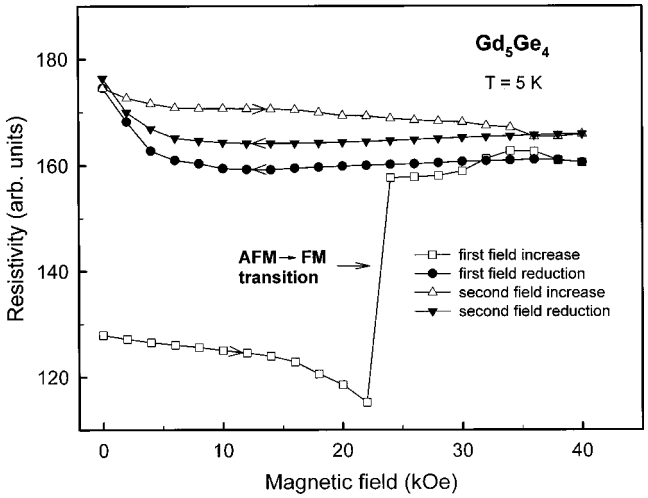

FIG. 5. Isothermal magnetic-field dependencies of the electrical resistivity of Gd_5Ge_4 at 5 K during cycling between 0 and 40 kOe.

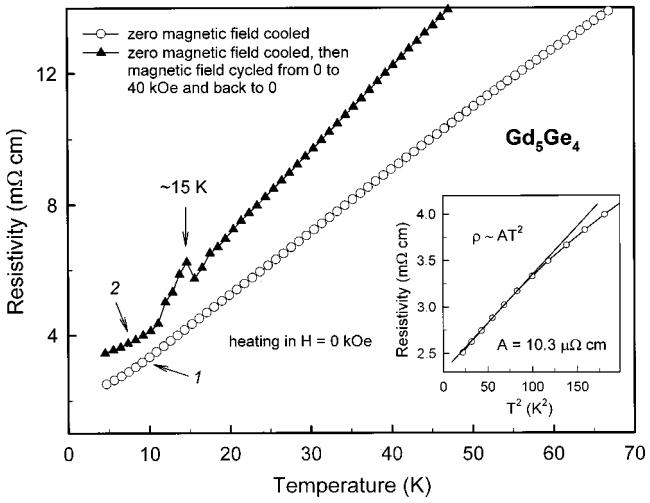

FIG. 6. Temperature dependencies of the electrical resistivity of Gd_5Ge_4 measured on heating in zero magnetic field after (1) the sample was cooled in zero magnetic field and was in the AFM state at 5 K; and (2) the sample was cooled in zero magnetic field and then held isothermally at 5 K while being subjected to a magnetic-field increase from 0 to 40 kOe and a reduction to 0, thus transforming the specimen into a FM state at 5 K. The inset shows the linear low-temperature behavior of the electrical resistivity in the AFM state from ~5 to ~16 K in $\rho \propto T^2$ coordinates in zero magnetic field.

The isothermal behavior of the electrical resistivity of Gd_5Ge_4, when the magnetic field was cycled between 0 and 40 kOe at 5 K, is presented in Fig. 5. When the magnetic field increases for the first time, the resistivity initially decreases, and then shows a sharp (~30%) discontinuity at ~22 kOe. This discontinuity corresponds to a transformation of Gd_5Ge_4 from an AFM into a FM state, as confirmed by the magnetic data. When the magnetic field is reduced from 40 kOe to zero, the resistivity remains nearly constant and then slightly increases below 5 kOe but the sharp discontinuity is no longer present. During the second and subsequent magnetic-field cycles (only the second cycle is shown in Fig. 5), the electrical resistivity shows no discontinuities because Gd_5Ge_4 remains ferromagnetic (as noted above). Therefore, the electrical resistivity of Gd_5Ge_4 is larger in the FM state when compared with that in the AFM state, and its behavior supports the conclusion that the metamagneticlike phase transition induced by a magnetic field at 5 K is irreversible.

The low-temperature dependencies of the electrical resistivity of Gd_5Ge_4 measured on heating in zero magnetic field without first applying magnetic field (curve 1), and also after the magnetic field was cycled between 0 and 40 kOe and back to zero at 5 K (curve 2), are shown in Fig. 6. The zero-magnetic-field resistivity of AFM Gd_5Ge_4 on heating and cooling shows a Fermi-liquid ($\rho \propto AT^2$) behavior[20,21] below 11 K (see the inset in Fig. 6) with $A = 10.3\ \mu\Omega\ \mathrm{cm/K^2}$. This is an unexpected result for a Gd-based material because this value of A falls into the category of the strongly correlated electron systems. For example, A is ~0.3 and ~40 $\mu\Omega\ \mathrm{cm/K^2}$ in the well-known representatives of strongly correlated electron systems V_2O_3 (Ref. 20) and $CeAl_3$,[21] respectively.

After the Gd_5Ge_4 sample is cycled in a magnetic field and the AFM state is irreversibly transformed into a FM state; the temperature dependence of the electrical resistivity shows a peak at ~15 K (Fig. 6). A similar peak is also observed at ~29 K when Gd_5Ge_4 is cooled in a 20-kOe dc magnetic field (Fig. 7). Therefore, regardless of whether Gd_5Ge_4 cooled in the nonzero magnetic field or heated after the magnetic field at 5 K increased from 0 to 40 kOe and reduced to zero again, the temperature change induces a first-order phase transition between the FM and AFM states. During these transformations, the electrical resistivity shows a peak reflecting the changes in the electronic structure of Gd_5Ge_4. The resistivity of Gd_5Ge_4, measured in an applied magnetic field both on heating and cooling, also shows a Fermi-liquid behavior (see the inset in Fig. 7). This behavior occurs over a broader temperature range (~5 to ~16 K) and with a smaller A (2.5

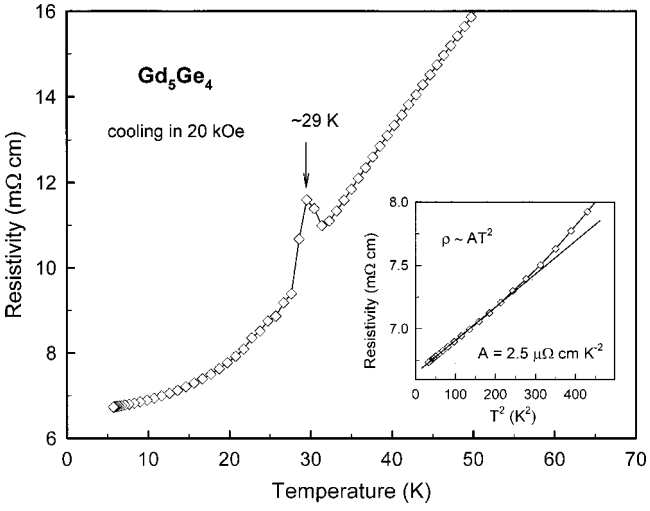

FIG. 7. Temperature dependence of the electrical resistivity of Gd_5Ge_4 measured on cooling in a 20-kOe magnetic field. The inset shows the linear low-temperature behavior of the electrical resistivity in the AFM state from ~5 to ~16 K in $\rho \propto T^2$ coordinates.

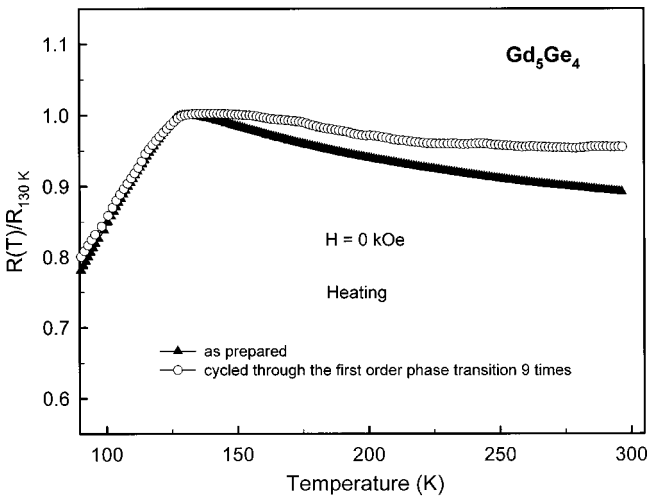

FIG. 8. Temperature dependencies of the electrical resistance of the Gd_5Ge_4 sample before and after it was cycled through the first-order phase transition nine times. To eliminate the difference due to an increase in ρ_0, the resistance was normalized to its maximum value at 130 K.

$\mu\Omega\,\mathrm{cm/K^2}$), when compared to that in zero magnetic field (see above).

The electrical resistivity of Gd_5Ge_4 is also quite different when compared with that of Gd_5Si_4.[22] The latter exhibits only a metallic behavior in both magnetically ordered and magnetically disordered states. We believe that this difference is due to the considerable differences in the interslab interactions[12,13,15] in both the silicide and the germanide, and thus a variation of the interslab bonding can significantly influence the electronic structure of these two compounds.

B. Electrical resistivity after the cycling of sample through the first-order phase transition

Simple thermal cycling of Gd_5Ge_4 between ~5 and ~300 K in zero magnetic field has no effect on its electrical resistivity both below and above 130 K. We note that during temperature cycling in zero magnetic field, Gd_5Ge_4 exhibits only a second-order magnetic phase transition at ~130 K, with no crystallographic phase change. A cycling of Gd_5Ge_4 through a first-order phase transition is possible by (1) increasing the magnetic field at 5 K to above ~20 kOe, and then heating the sample in zero magnetic field to above ~15 K; (2) heating and cooling in magnetic fields exceeding ~20 kOe; and/or (3) magnetizing and demagnetizing the sample at 25–35 K using a magnetic field on the order of ~40 kOe.[14] As a result of cycling through the first-order phase transition, the electrical resistivity of Gd_5Ge_4 changes. First, the total electrical resistivity continuously increases, which is expected due to the reported[13,15] volume change and the appearance of additional microcracks in the sample.[9,23] Second, the low-temperature metalliclike behavior of the electrical resistivity of Gd_5Ge_4, i.e., below 130 K, remains similar, but the high-temperature semiconductorlike behavior, i.e., above 130 K, changes considerably. Figure 8 shows this change by comparing the high-temperature dependencies of the electrical resistivity of the as prepared Gd_5Ge_4 sample and after it was cycled through the first-order phase transition nine times. The observed change in the $\rho(T)$ slope indicates that the resistivity of the high-temperature nonmetallic state of Gd_5Ge_4 is quite sensitive to microcracks in the specimen. One can assume that lattice defects, which appear during the cycling, result in a less pronounced localization of the charge carriers, which is manifested through the less negative $d\rho/dT$ in the paramagnetic, nonmetallic region.

C. Possible models for the observed behavior of the electrical resistivity

In general, the main contributions to the zero-magnetic-field electrical resistivity of metallic Gd-based magnetic alloys arise from the residual resistivity (ρ_0), phonon scattering (ρ_{ph}), electron scattering (ρ_{el}), and magnetic scattering (ρ_{mag}). However, the behavior of the electrical resistivity of Gd_5Ge_4 is quite different when compared with other common Gd-based compounds.[5–7,24,25] First, in the high-temperature paramagnetic state, the electrical resistivity has a negative $d\rho/dT$, and is larger than Mott's limit for the metallic resistivity, which is about $\rho_{\max}=\sigma_{\min}^{-1}=(e^2n/\hbar k_F^2)^{-1}$ $\approx 1\,\mathrm{m}\Omega\,\mathrm{cm}$.[18] Second, the electrical resistivity of Gd_5Ge_4 shows an irreversible change at 5 K induced by a magnetic field due to a metamagneticlike transition. Finally, after Gd_5Ge_4 has been irreversibly transformed into the ferromagnetic state at 5 K, its electrical resistivity exhibits a peak during heating in zero magnetic field and a similar peak during cooling in an applied magnetic field, showing that the electrical resistance is quite sensitive to phase transitions between AFM and FM phases (in the majority of Gd-based compounds such a transition is generally manifested as a change in slope in a resistivity vs temperature plot).

In the metallic Gd,[26] as well as in other Gd-based metallic materials,[1,9] the contribution of magnetic disorder to the electrical resistivity is similar in different materials, assuming that it has a nearly linear temperature dependence in the ferromagnetic state. The magnetic disorder contribution reaches its maximum in the paramagnetic state due to the maximum disorder of the localized magnetic moments. Because the electrical resistivity of Gd_5Ge_4 does not show a metallic behavior in the paramagnetic state, it is impossible to determine the real value of ρ_{mag} by an approximation of the pure electron-phonon component to 0 K. However, since Gd_5Ge_4 is clearly paramagnetic above ~130 K, and assuming a magnetic contribution coefficient of ~0.38 $\mu\Omega\,\mathrm{cm/K}$,[1,26] we obtain a maximum of $\rho_{\mathrm{mag}}\approx 50\,\mu\Omega\,\mathrm{cm}$, which is more than two orders of magnitude smaller than the experimentally observed resistivity at 130 K. Therefore, the presence of only ρ_{ph} and ρ_{mag} contributions does not provide an explanation for the unusually large $\Delta\rho/\rho\Delta T\approx 10^{-2}\,\mathrm{K}^{-1}$ of Gd_5Ge_4 in the temperature range from 4.3 to 130 K.

Since the temperature dependence of the electrical resistivity is determined by both the mobility of the charge carriers and their concentration, a change of one or both during the phase transformation in Gd_5Ge_4 is quite likely. In principle, the anomalous reduction of the electrical resistivity in lanthanide metallic systems with temperature can be the re-

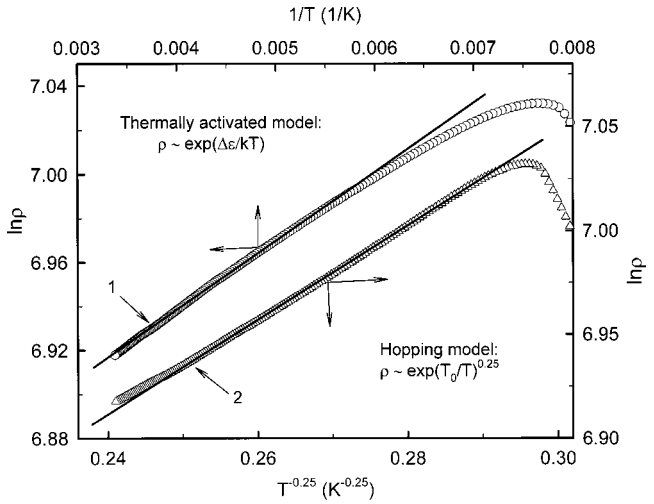

FIG. 9. Temperature dependencies of the electrical resistivity of Gd_5Ge_4 plotted in the $\ln\rho \propto 1/T$ (curve 1) and $\ln\rho \propto T^{-0.25}$ (curve 2) coordinates.

sult of various reasons: (1) Kondo scattering [$\rho \propto \ln T$] due to the strong $4f$-$s(d$-) correlations, e.g., heavy fermion systems;[1,3] (2) thermally activated generation of charge carriers [$\rho \propto \exp(\Delta\varepsilon/kT)$] in the system where their low-temperature concentration is lower than in metals, which is usually observed in materials with an energy gap in the electronic structure (i.e., semiconductors), or in materials with weakly overlapping valence and conduction bands (i.e., semimetals); and (3) a hopping process [$\rho \propto \exp(T_0/T)$] usually observed in atomically and/or magnetically disordered metallic materials.[18]

Considering the first possibility outlined above, it is unlikely that the negative $d\rho/dT$ above ~130 K in Gd_5Ge_4 is the result of interactions between the localized $4f$ electrons of Gd and conduction electrons. Such a behavior is observed in Ce-, Eu-, and Yb-based metallic materials, where similar anomalies were observed at low temperatures and are due to the intra-atomic and interatomic electrons correlation.[1] Furthermore, the experimental temperature dependence of the electrical resistance of Gd_5Ge_4 cannot be fitted by the $\rho \propto \ln T$ law over the entire temperature range above 130 K.

Considering the second possible mechanism, it is possible that an energy gap appears in the electronic structure of Gd_5Ge_4 above 130 K. The observed temperature dependence of the electrical resistance of Gd_5Ge_4 can be linearly approximated in the $\ln\rho \propto 1/T$ coordinates above ~140 K (see Fig. 9). Assuming that in this region a true thermally activated process takes place, the calculated energy gap is about 5.4 meV. However, a system with such a small energy gap in the electronic structure is expected to be degenerate at temperatures above ~70 K and a semiconductorlike behavior, therefore, should not be observed.

Considering the third possible mechanism, we find that the electrical resistivity above ~130 K measured on both heating and cooling can also be fitted by the expression $\rho \propto \exp(T_0/T)''$, which usually describes the electrical resistivity in terms of the hopping model.[18,27] Certainly, due to the limited temperature range, the T_0/T ratio is rather small for the correct determination of n, but Fig. 9 shows that $n = 0.25$ may reasonably describe the temperature dependence of the electrical resistivity of Gd_5Ge_4 above 130 K. To suggest the hopping process as the possible mechanism of the electrical conductivity in Gd_5Ge_4, one can assume that above $T_{MIT} \approx 130$ K the conduction electrons in Gd_5Ge_4 are temporarily trapped by the localized electronic states of the nonbonded Ge atoms located on the slab surfaces, i.e., they form electronic pairs with partially unfilled valence atomic orbitals. Therefore, this trapping is responsible for a reduction of the electrical conductivity of the material. In principle, this model is similar to the model proposed to explain the electron-phonon coupling in the colossal magnetoresistance manganites which is strong enough to ''self-trap'' the conduction electrons, producing a truly insulating state at high temperatures.[28,29] Also, this model finds support in the behavior of the electrical resistance of other $Gd_5(Si_xGe_{4-x})$ materials which have a nonmetallic character in the paramagnetic state with nearly zero $d\rho/dT$[9] for $Gd_5(Si_2Ge_2)$, where only one-half of the interslab bonds remains, or the metallic character with a positive $d\rho/dT$[17,22] for Gd_5Si_4, where all interslab bonds are present. The hopping model, therefore, seems the most likely mechanism responsible for the anomalous reduction of the electrical resistivity of Gd_5Ge_4 above ~130 K.

Regardless of the actual mechanism, we should note that the MIT observed in Gd_5Ge_4 at ~130 K is the result of a change in the electronic structure, and that change coincides with the transition between the low-temperature (<130 K) antiferromagnetic and high-temperature (>130 K) paramagnetic states. In general, metal-insulator transitions can be divided into two categories:[30,31] Mott-Hubbard transitions triggered by electronic correlations, and Anderson-Mott transitions triggered by a disorder. It is difficult to completely understand the nature of the metal-insulator transition in Gd_5Ge_4 without the availability of low-temperature crystallographic and magnetic structure data. However, it is clear that the metal-insulator transition in Gd_5Ge_4 is accompanied by an order↔disorder magnetic phase transition, and it is feasible that the temperature-induced change of the lattice parameters (i.e., thermal expansion) may play an important role in this transition by changing interatomic distances. The temperature dependencies of the heat capacity of Gd_5Ge_4 in zero and nonzero magnetic fields show that the metal-insulator transition occurring in Gd_5Ge_4 is a second-order phase transition, and the temperature of this transition changes from ~130 K in zero magnetic field to ~115 K in 100-kOe magnetic field.

Furthermore, although Gd_5Ge_4 is not ferromagnetic at low temperatures in zero magnetic field, and there is no interaction between the slabs propagating through Ge-Ge bonds, the metallic state can appear below ~130 K due to the change in the overlap or in localization of the $5d$ electronic orbitals of Gd. However, we believe that due to larger interatomic distances, the overlap of these $5d$ orbitals in Gd_5Ge_4 is smaller when compared with Gd_5Si_4 and it is feasible that at low temperatures Gd_5Ge_4 is a metal with a narrow conduction band.

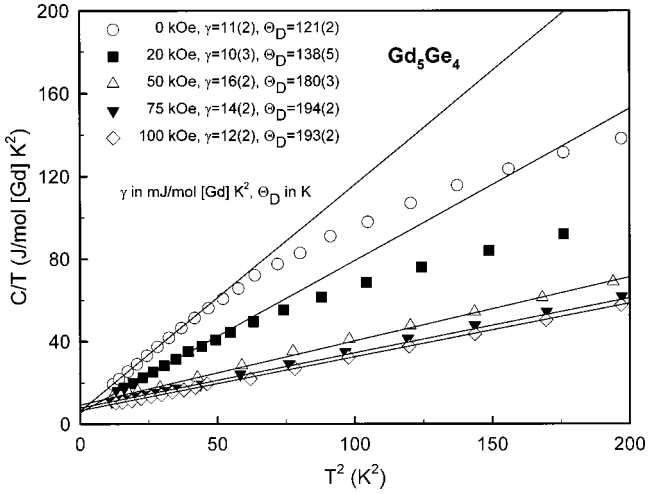

FIG. 10. The C/T vs T^2 dependence of Gd_5Ge_4 from 3.5 to ~14 K. The symbols represent experimental data points, and solid lines indicate the results of a least-squares fit of the experimental data using $C=\gamma T+\beta T^3$.

D. Electronic specific-heat coefficient

If our suggestion about the appearance of a narrow conduction band below 130 K is true, an increased effective mass of the conduction electrons, i.e., an enhancement of both the density of states at the Fermi level and, therefore, the Sommerfeld specific-heat coefficient, should be also observed. The low-temperature dependencies of the C/T vs T^2 function of Gd_5Ge_4 in zero and nonzero magnetic fields, the calculated electronic specific-heat coefficients (γ) and Debye temperatures (Θ_D) are presented in Fig. 10. The average electronic heat-capacity coefficient, $\gamma=13\pm3$ mJ/mol[Gd] K^2, is enhanced when compared with that for many other metallic systems with weak electron correlations. Furthermore, according to our data the electronic specific-heat constants for Gd_5Si_4 and La_5Ge_4 are 2.5 mJ/mol[Gd] K^2 and 3.2 mJ/mol[La] K^2, respectively. The temperature interval, where C/T has a linear temperature dependence, increases with a magnetic field, i.e., between 3.5 and ~7 K in zero magnetic field, and between 3.5 and ~14 K for $H\geqslant 50$ kOe (Fig. 10). The enhancement of the electronic heat capacity, therefore, supports the presence of a narrow conduction band in Gd_5Ge_4 at low temperatures.

It is evident from Fig. 10 that there is a significant difference in the slope (β) of the C/T vs T^2 plots for the zero-field results and for the magnetic-field results for $H\geqslant 50$ kOe, with the 20-kOe data lying between the two sets of functions. Since β is inversely related to the Debye temperature, as follows from

$$\Theta_D^3=(1/\beta)1.9437\times10^6, \tag{1}$$

we will discuss the observed behavior in terms of the Debye temperature. In zero magnetic field the Debye temperature of antiferromagnetic Gd_5Ge_4 is 121 K, which is significantly lower than that observed for ferromagnetic Gd_5Si_4 (241 K) and for paramagnetic La_5Ge_4 (192 K). We note that in both Gd_5Si_4, which has interslab bonds, and La_5Ge_4, which has no interslab bonds, the Debye temperature is magnetic field independent. Furthermore, the high magnetic field Θ_D for Gd_5Ge_4 is 189 ± 3 K, which is consistent with the Θ_D value for La_5Ge_4 and somewhat low compared to Gd_5Si_4. In order to make a more meaningful comparison, we make use of the Lindemann equation[32] relating Θ_D to the melting point T_m, the molar mass M, and the atomic volume V,

$$\Theta_D=K(T_m/M)^{1/2}(1/V)^{1/3}, \tag{2}$$

where K is a constant. Using the measured Θ_D of Gd_5Si_4, we can determine K and then estimate what the Θ_D values might be for Gd_5Ge_4 and La_5Ge_4, assuming Lindemann's equation holds. The calculated value for La_5Ge_4 is 190 K, which is in excellent agreement with the observed value of 192 K. But for Gd_5Ge_4 the calculated value of 214 K is about 12% larger than the measured value of 189 K. This difference is probably within the reliability of Eq. (2).

The zero field Θ_D of Gd_5Ge_4 (121 K) is another matter; it is much too low compared to the values for the other R_5X_4 phases. This suggests that there is a magnetic contribution to the observed slope, i.e., $\beta_T=\beta_L+\beta_M$, where the subscripts denote the following: T total; L lattice; and M magnetic. This is quite reasonable since Gd_5Ge_4 orders antiferromagnetically in zero magnetic field below 128 K; see Fig. 4. For a simple antiferromagnetic material $C_M\propto T^3$ (Ref. 33), which would account for a nonzero β_M value, and thus a larger β_T. At $H=20$ kOe (applied at the lowest temperature, i.e., ~3.5 K) the Gd_5Ge_4 is a two-phase material consisting of antiferromagnetic and ferromagnetic structures,[14] and therefore the observed Θ_D (138 K) is intermediate between zero (121 K) and high-field values (189 K).

Although, as discussed above, in magnetic fields below ~50 kOe the calculated values of the Debye temperature (from the heat capacity) are biased by magnetic excitations, we believe that there may be another contribution to the observed steplike increase of Debye temperature of Gd_5Ge_4 between 0 and 50 kOe. It is possible that the phonon excitations change due to the crystallographic phase change and the formation of the interslab bonds, which could account for some of the increases in Θ_D.

E. Calculated electronic structure of Gd_5Ge_4

To gain some insights into the metal-semiconductor transition in Gd_5Ge_4, tight-binding linear-muffin-tin-orbital calculations using the atomic sphere approximation (TB-LMTO-ASA)[34,35] were carried out using the available information about the room-temperature crystal structure and a model of the low-temperature structure based on low-temperature crystallographic parameters for $Gd_5(Si_{0.33}Ge_{3.67})$, in which all Si and Ge atoms belong to dimers (of Gd_5Si_4 type).[12,36] The basis set for the TB-LMTO-ASA calculations consisted of $6s$, $6p$, $5d$, and $4f$ functions for Gd (Wigner-Seitz radii between 3.3 and 3.5 atomic units) and $4s$, $4p$, and $4d$ functions for Ge (a Wigner-Seitz radius of 2.9 atomic units). Also, to satisfy the overlap criteria of atomic spheres in the LMTO-ASA method, 52 empty spheres were included in the unit cells. k-space integrations were made using the tetrahedron method, with more than 1000 k

points within the irreducible wedges of the first Brillouin zones to calculate the energy densities of states (DOS). In addition to the room-temperature calculation, magnetically disordered state, spin-polarized calculations were performed for the magnetically ordered states for both the low temperature [i.e., Gd_5Si_4-type; see Fig. 1(b)] and room-temperature [i.e., Sm_5Ge_4-type; see Fig. 1(a)] crystal structure models.

Figure 11 illustrates the total DOS curves for the three cases calculated in this study: (a) room-temperature, magnetically disordered Gd_5Ge_4 (only valence *s*, *p*, and *d* functions are included here, since the $4f$ functions are treated as valence orbitals in this model, which form a narrow, intense peak at the Fermi level, and thus would obscure the valence *s*, *p*, and *d* bands in this energy region); (b) room-temperature, magnetically ordered Gd_5Ge_4; and (c) low-temperature, magnetically ordered Gd_5Ge_4 (for spin-polarized models, majority- and minority-spin DOS curves are separated). For the magnetically ordered models, (b) and (c), the narrow Gd $4f$ bands are split by ~5.5 eV with the majority-spin $4f$ states ~4.5 eV below the Fermi level and the minority-spin $4f$-states 1.1 eV above the Fermi level. The net numbers of unpaired electrons at the Gd and Ge sites range, respectively, from 7.06–7.20 and 0.00–0.03 electrons. Common features to all three curves include (i) states between −10.8 and −7.0 eV, which are mostly Ge $4s$ levels; (ii) states between approximately −5.0 eV to just below the Fermi level, which have significant combinations of Ge $4p$ and Gd $6s$ and 5d orbitals; (iii) states just above the Fermi level which are largely Gd $6s$ and $5d$ orbitals; and (iv) the DOS curves for all cases, except that the majority-spin bands of the room temperature magnetically ordered model (b) show a small energy gap a few tenths of an eV below the Fermi level.

To achieve insights into the changes in the electronic structure, which may account for the observed transport behavior of Gd_5Ge_4, requires a focus on the states near the Fermi level. Figure 12 shows the *spd*-only DOS curves for all three cases for a 5-eV window near the Fermi level. These curves also show the contributions from Gd $6s$, $6p$, and $5d$ states in this region, which suggests there are significant combinations from the Gd and Ge valence orbitals. Furthermore, the Fermi levels for the magnetically ordered models show nonzero densities of states, which is consistent with the metallic behavior of the low-temperature form of Gd_5Ge_4; whereas the Fermi level for the magnetically disordered model falls in the middle of a very narrow set of bands which suggests the possibility of a Mott-Hubbard semiconducting behavior for this phase.

1. Room-temperature, magnetically disordered model

The calculated Fermi level of −1.30 eV intersects a very narrow, distinguishable band (the bandwidth is ~70 meV) of four orbitals per unit cell [Fig. 12(a)]. The DOS curve falls to zero at approximately −1.40 eV and these occupied states correspond to 15 valence *s*, *p*, and *d* states per Gd_5Ge_4 formula unit. In a formal sense, the 30 valence electrons occupying these states can be assigned to Ge $4s$ and $4p$ orbitals (although this is a drastic simplication as seen by the Gd partial DOS). According to the room-temperature structure

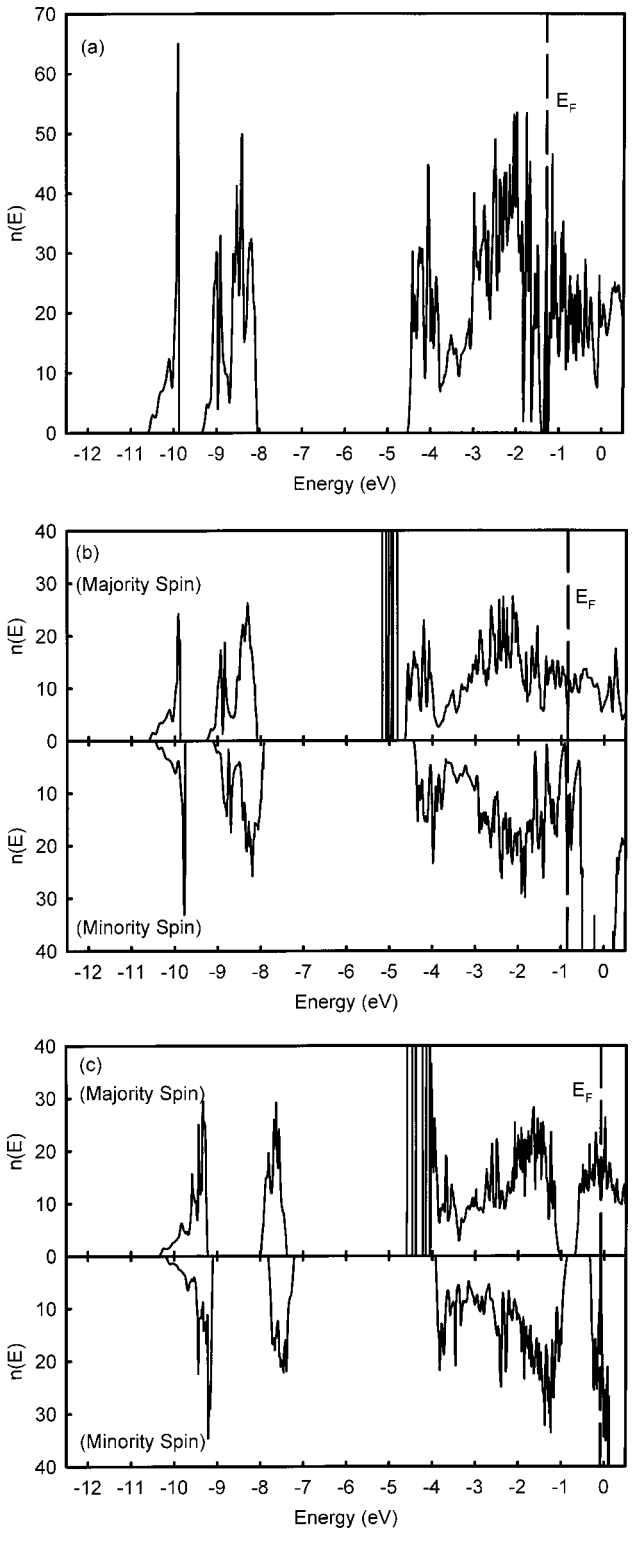

FIG. 11. Total DOS curves in the energy range −12.5 to 0.5 eV for different models of Gd_5Ge_4: (a) room-temperature, magnetically disordered model (only the *s*-, *p*- and *d*- valence orbital contributions are shown); (b) room-temperature, magnetically ordered model; and (c) low-temperature, magnetically ordered model (see the text for the structural model used). In (b) and (c), the majority- and minority-spin DOS curves are separated, and the Gd $4f$-orbital contributions are included. The vertical dashed lines in each graph indicate the corresponding Fermi levels (E_F).

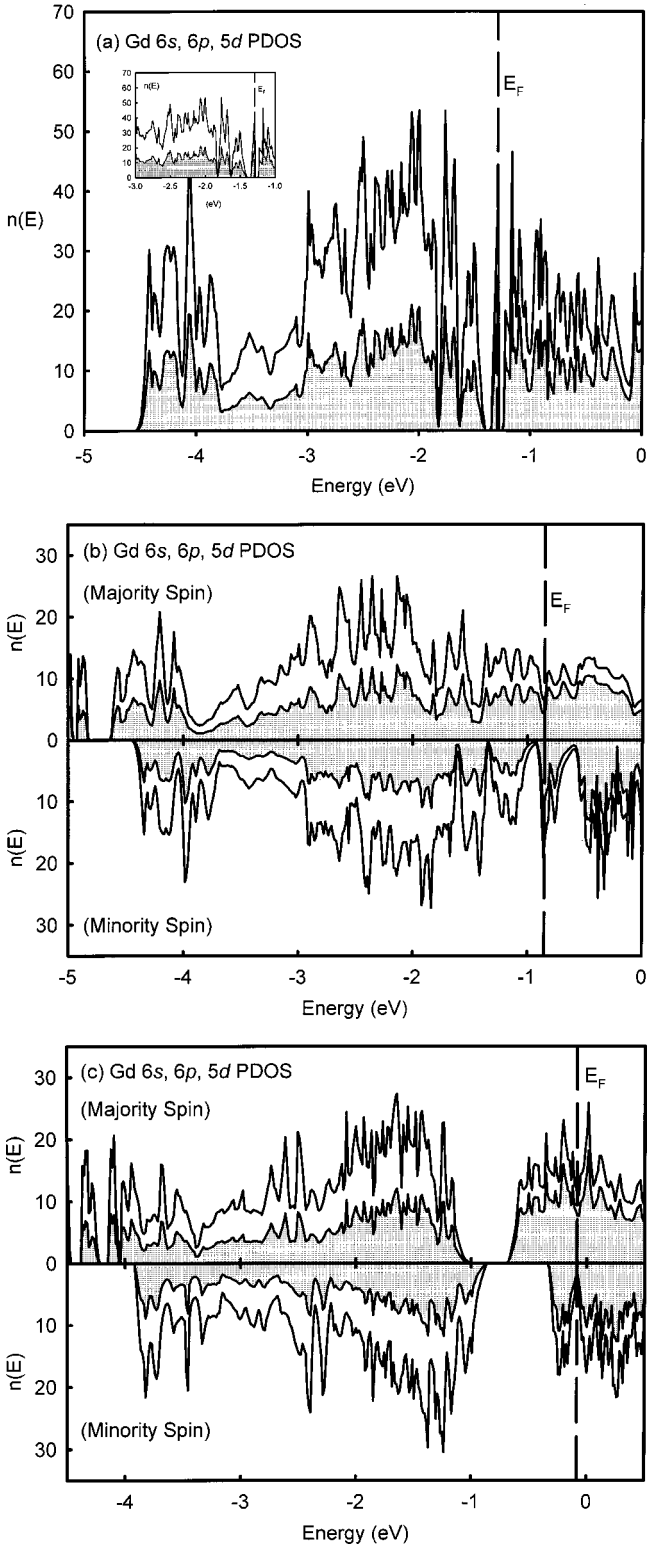

FIG. 12. Valence *s*, *p*, and *d* DOS curves in a 5.0-eV energy window near the corresponding Fermi levels for each of the three models, [(a), (b), and (c)]. The partial DOS (PDOS) contributions from Gd are shaded. The inset in (a) shows a 2.0-eV window to highlight the distinct, narrow band that is the highest occupied valence band in the magnetically disordered model.

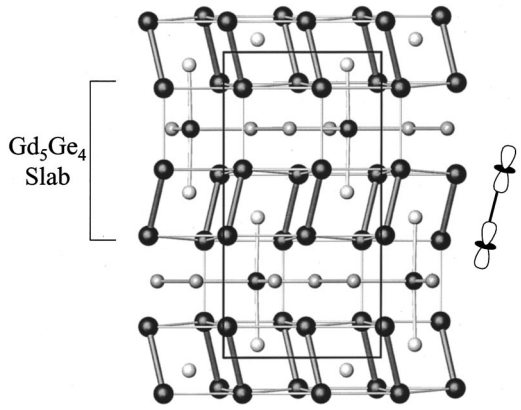

FIG. 13. Projection of the room-temperature structure of Gd_5Ge_4 along the [001] direction emphasizing the Gd-Gd interactions (dark lines) between the slabs that contribute to the half-occupied band in the DOS of the magnetically disordered model (a). The nature of the orbital is illustrated schematically at the right. The small, light circles represent Ge atoms, and the large, dark circles the Gd atoms.

of Gd_5Ge_4, the chemical formula can be rewritten $Gd_5(Ge_2)(Ge_2)$, which emphasizes that 50% of the Ge atoms [i.e., the atoms located inside the slabs; see Fig. 1(a)] form chemically distinct dimers (the Ge-Ge distance is 2.688 Å) while 50% [i.e., those found on the slab surface; see Fig. 1(a)] do not. According to the Zintl-Klemm electron counting formalism for valence compounds,[37] the Ge_2 dimers are counted as isoelectronic with halogen dimers, i.e., seven electron pairs, and each isolated Ge atom is counted as isoelectronic with a noble-gas atom, i.e., four electron pairs. This formalism accounts for the 15 electron pairs per formula unit needed to occupy states up to -1.40 eV in the DOS curve of this model.

Since Gd_5Ge_4 has 31 valence electrons per formula unit, the additional electron will occupy the narrow band at approximately -1.30 eV. According to the band structure, as well as the integration of the DOS curve, this narrow band consists of four crystal orbitals. Since there are four formula units per unit cell, this band is half-filled by four valence electrons. The DOS curve shows that it splits away from the conduction band by $\sim$50 meV. An analysis of the four crystal orbitals at the Γ point shows a structural rationale for this observed narrow band: although the Ge-Ge distance (3.588 Å) between the $[Gd_5Ge_4]$ slabs precludes a strong chemical interaction between Ge atoms, there is a short Gd-Gd contact (3.532 Å) between these slabs. The four crystal orbitals arise from four Gd-Gd σ-bonding orbitals formed from $5d\text{-}z^2$ orbitals along the ''bond'' axes. Weak orbital interactions along the three crystallographic directions maintain a weak dispersion throughout reciprocal space. Figure 13 illustrates the room-temperature crystal structure of Gd_5Ge_4 [i.e., the same as in Fig. 1(a)], and identifies the short Gd-Gd contacts that contribute to the narrow band in question. With four valence electrons per unit cell available, this narrow band would be half-filled to create a nonmetallic behavior in the sense of a Mott-Hubbard semiconductor. This theoretical result supports, in principle, the thermally activated mechanism that

was considered above in Sec. III C, in which the various models for electron transport were discussed. The presence of the small energy gap in the *spd* electronic structure of Gd_5Ge_4 also agrees with available data from x-ray photoelectron spectra.[38] It is noted that the space group for the room-temperature Gd_5Ge_4, *Pnma* requires fourfold degeneracies in the one-electron energy band diagram, e.g., at points $Y(\mathbf{b}^*/2)$, $S(\mathbf{a}^*/2+\mathbf{b}^*/2)$, and $R(\mathbf{a}^*/2+\mathbf{b}^*/2+\mathbf{c}^*/2)$. Since the unit cell of Gd_5Ge_4 contains 124 valence *s*, *p*, and *d* electrons, the highest occupied one-electron energy bands must be partially occupied. Therefore, the semiconducting behavior in Gd_5Ge_4 cannot arise from the completely filled energy bands separated by an energy gap from the conduction band.

2. Room-temperature, magnetically ordered model

The DOS curve [Fig. 12(b)] shows that this model would lead to a metallic behavior due to the nature of the majority-spin states, even through the Fermi level at -0.85 eV lies in a local minimum. On the other hand, there is a small fraction of a narrow, ~350 meV wide, band occupied in the minority-spin DOS curve. This noticeable peak in the DOS corresponds to the four σ-bonding $5d\text{-}z^2$ orbitals identified in the magnetically disordered model. Subtle changes in structure, as may occur on cooling, could lead to shifts of these states in the DOS curves, and Gd_5Ge_4 could become ''insulator-like,'' which has been reported for *T*MnSb (*T*=Fe, Co, Ni, and Pt) phases.[39]

3. Low-temperature, magnetically ordered model

According to the DOS curve [Fig. 12(c)], this model is clearly metallic. But, in both the majority- and minority-spin DOS curves, the Fermi level at -0.08 eV falls in a local minimum. It is noted that the energy gap near -1.0 eV separates 14 occupied states below from the conduction band above. According to the formulation of this low-temperature structure, $Gd_5(Ge_2)_2$, where all Ge atoms form chemically distinct dimers [see Fig. 1(b)], each Ge_2 dimer requires seven occupied orbitals, which accounts (formally) for the observed gap in the DOS curves. In this structure, however, the shortest Gd-Gd contact increases from 3.52 Å in the magnetically disordered phase to ~3.75 Å in the low-temperature magnetically ordered phase, and the distinct, narrow band associated with the room temperature structure, [models (a) and (b)] now overlaps the conduction band.

Although these computational results provide a model for the changes in the electronic transport of Gd_5Ge_4 that is consistent with experimental observations, they also represent a preliminary effort to identify and understand the complex interplay among the crystal structures, electronic transport, and magnetic properties in this system. Further theoretical and experimental studies, especially taking into account the complex magnetic behavior of Gd_5Ge_4 (see Sec. III A and Fig. 4) are underway.

IV. CONCLUSIONS

Gd_5Ge_4 exhibits several interesting electronic transport phenomena including a high-temperature metal-insulator-like phase transition and a low-temperature first-order phase transition induced by a magnetic field. We show that the observed behavior of the electrical resistance of Gd_5Ge_4 is determined by several mechanisms, i.e., by (1) the magnetic-field-induced metamagnetic transition, and (2) the temperature-induced transition between metallic and nonmetallic states. Both the Fermi-liquid behavior of the electrical resistivity of Gd_5Ge_4 and the electronic heat capacity indicate the presence of a narrow conduction band with strong electron correlations at low temperatures. Several models, which can describe the electrical resistivity of Gd_5Ge_4 above $T_{MIT}\approx 130$ K, have been considered, and a hopping model seems to best explain the observed behavior. Preliminary tight-binding linear-muffin-tin-orbital calculations indicate that Gd_5Ge_4 may behave as a metal in the magnetically ordered state at low temperature and as a Mott-Hubbard semiconductor at high temperature in the magnetically disordered state.

ACKNOWLEDGMENTS

The Ames Laboratory is operated for the U.S. Department of Energy by Iowa State University under Contract No. W-7405-ENG-82. This work was supported by the Office of Basic Energy Sciences, Materials Sciences Division, of the U.S. Department of Energy.

*Corresponding author. Present address: 242 Spedding, Ames Laboratory, Iowa State University, Ames, Iowa 50011-3020, Email address: vitkp@ameslab.gov, Fax: (515) 294-9579

[1] D. Wohlleben and B. Wittershagen, Adv. Phys. **34**, 403 (1985).
[2] J. Pierre, S. Auffret, J. A. Chroboczek, and T. T. A. Nguyen, J. Phys.: Condens. Matter **6**, 79 (1994).
[3] R. P. van Gorkom, A. Brataas, and G. E. W. Bauer, Phys. Rev. Lett. **83**, 4401 (1999).
[4] D. L. Cox and A. Zawadowski, Adv. Phys. **47**, 599 (1998).
[5] S. R. Saha, H. Sugawara, T. D. Matsuda, and H. Sato, Phys. Rev. B **60**, 12 162 (1999).
[6] S. Majumdar and E. V. Sampathkumaran, Phys. Rev. B **61**, 43 (2000).
[7] P. A. Stampe, X. Z. Zhou, H. P. Kunkel, J. A. Cowen, and G. Williams, J. Phys.: Condens. Matter **9**, 3763 (1997).
[8] L. Morellon, P. A. Algarabel, M. R. Ibarra, J. Blasco, B. García-Landa, Z. Arnold, and F. Albertini, Phys. Rev. B **58**, R14 721 (1998).
[9] E. M. Levin, V. K. Pecharsky, and K. A. Gschneidner, Jr., Phys. Rev. B **60**, 7993 (1999).
[10] V. K. Pecharsky and K. A. Gschneidner, Jr., Phys. Rev. Lett. **78**, 4494 (1997).
[11] F. Holtzberg, R. J. Gambino, and T. R. McGuire, J. Phys. Chem. Solids **28**, 2283 (1967).
[12] V. K. Pecharsky and K. A. Gschneidner, Jr., J. Alloys Compd. **260**, 98 (1997).
[13] W. Choe, V. K. Pecharsky, A. O. Pecharsky, K. A. Gschneidner, Jr., V. G. Young, Jr., and G. J. Miller, Phys. Rev. Lett. **84**, 4617 (2000).

[14] E. M. Levin, V. K. Pecharsky, and K. A. Gschneidner, Jr. (unpublished).
[15] L. Morellon, J. Blasco, P. A. Algarabel, and M. R. Ibarra, Phys. Rev. B **62**, 1022 (2000).
[16] V. K. Pecharsky, J. O. Moorman, and K. A. Gschneidner, Jr., Rev. Sci. Instrum. **68**, 4196 (1997).
[17] J. Szade and G. Skorek, J. Magn. Magn. Mater. **196–197**, 699 (1999).
[18] N. F. Mott, *Metal-insulator Transitions* (Taylor & Francis, London, 1974), p. 278.
[19] H. Kawamura, J. Phys.: Condens. Matter **10**, 4707 (1998).
[20] W. Bao, C. Broholm, G. Aeppli, S. A. Carter, P. Dai, C. D. Frost, J. M. Honig, and P. Metcalf, J. Magn. Magn. Mater. **177–181**, 283 (1998).
[21] U. Rauchschwalbe, Physica B&C **147**, 1 (1987).
[22] Yu. V. Serdyuk, R. P. Krentsis, P. V. Gel'd, and V. G. Batalin, Fiz. Tverd. Tela (Leningrad) **22**, 2149 (1980) [Sov. Phys. Solid State **22**, 1251 (1980)].
[23] L. Morellon, J. Stankiewicz, B. García-Landa, P. A. Algarabel, and M. R. Ibarra, Appl. Phys. Lett. **73**, 3462 (1998).
[24] G. Chelkowska, J. Alloys Compd. **209**, 337 (1994).
[25] E. V. Sampathkumaran and I. Das, Phys. Rev. B **51**, 8631 (1995).
[26] R. V. Colvin, S. Legvold, and F. H. Spedding, Phys. Rev. **120**, 741 (1960).
[27] J. M. D. Coey, M. Viret, L. Ranno, and K. Ounadjela, Phys. Rev. Lett. **75**, 3910 (1995).
[28] A. J. Millis, P. B. Littlewood, and B. I. Shraiman, Phys. Rev. Lett. **74**, 5144 (1995).
[29] A. J. Millis, J. Appl. Phys. **81**, 5502 (1997).
[30] D. Belitz and T. R. Kikpatrick, Rev. Mod. Phys. **66**, 261 (1994).
[31] M. Imada, A. Fujimori, and Y. Tokura, Rev. Mod. Phys. **70**, 1039 (1998).
[32] F. A. Lindemann, Phys. Z. **11**, 609 (1910).
[33] E. S. R. Gopal, *Specific Heats at Low Temperatures* (Plenum, New York, 1966), p. 89.
[34] O. K. Andersen and O. Jepsen, Phys. Rev. Lett. **53**, 2571 (1984).
[35] O. K. Andersen, Z. Pawlowska, and O. Jepsen, Phys. Rev. B **34**, 5253 (1986).
[36] G. J. Miller, W. Choe, M. Wöhrle, A. O. Pecharsky, K. A. Gschneidner, Jr., and V. K. Pecharsky (unpublished).
[37] G. J. Miller, in *Chemistry, Structure and Bonding of Zintl Phases and Ions*, edited by S. M. Kauzlarich (VCH, New York, 1996), p. 1.
[38] J. Szade and M. Neuman, J. Phys.: Condens. Matter **11**, 3887 (1999).
[39] R. A. de Groot, F. M. Mueller, P. G. van Engen, and K. H. J. Buschow, Phys. Rev. Lett. **50**, 2024 (1983); D. T. Pierce, and F. Meier, Phys. Rev. B **13**, 5484 (1976); R. A. de Groot, A. M. van der Kraan, and K. H. J. Buschow, J. Magn. Magn. Mater. **61**, 330 (1986); R. A. de Groot, Physica B **172**, 45 (1991).